detritus | Multidisciplinary Journal for Circular Economy and Sustainable Management of Residues

CISA

PRELIMINARY EXPERIMENTAL STUDY ON GREEN DIESEL PRODUCTION WITH REDUCED IMPACT OF SOLVENT

Sonia Dell'Aversano [1,*], Katia Gallucci [1], Giuseppina Vanga [2], Andrea Di Giuliano [1], Giuseppe Di Vito Nolfi [3], Leucio Rossi [3] and Carlo Villante [1]

[1] *Department of Industrial and Information Engineering and Economics, University of L'Aquila, Monteluco diRoio, 67100 L'Aquila, Italy*
[2] *ENEA, Italian National Agency for New Technologies, Energy and Sustainable Economic Development, via Anguillarese 301, 00123 Rome, Italy*
[3] *Department of Physical and Chemical Sciences, University of L'Aquila, via Vetoio (Coppito), 67100 L'Aquila, Italy*

Article Info:
Received:
16 June 2025
Revised:
13 October 2025
Accepted:
3 November 2025
Available online:
11 December 2025

Keywords:
Green diesel
Deoxygenation process
Solvent minimization
Ni-Mo-Al catalyst
Triglyceride conversion
Product selectivity

ABSTRACT

This study inverstigates the catalytic deoxygenation (DO) of rapeseed oil for the production of green diesel, focusing on minimizing environmental impact through solvent reduction in accordance with green chemistry and green engineering principles. A series of batch-scale experiments was performed using a novel Ni-Mo-Al catalyst (MOM), synthesized via a new solvent-free method (under patenting procedure) and applied in combination with a process strategy to reduce solvent usage in the DO reaction. Reactions were conducted under varying n-hexane:oil mass ratios (10:1 to 4:1) and oil loadings (2-5 g) to assess the compromise between solvent use and process performance. Key metrics–triglyceride conversion, diesel-range hydrocarbon yield, and product composition–were evaluated by gas chromatography. The optimal condition (4:1 n-hexane:oil mass ratio, 3 g oil loading) resulted in over 99% triglyceride conversion and a 74.2 wt% diesel yield, with more than 90% of the hydrocarbon fraction falling within the C_{15}-C_{18} range. Product selectivity across all tests favored decarboxylation and decarbonylation over hydrodeoxygenation. Notably, the MOM catalyst showed high activity despite solvent reduction in the DO environment, providing a preliminary yet promising demonstration of how solvent-free catalyst design and solvent minimization can jointly advance more sustainable green diesel production.

1. INTRODUCTION

The Earth's climate system is governed by complex interactions that have been increasingly disrupted by anthropogenic emissions of greenhouse gases (GHGs) (Baede et al., 2022). While climate variability has occurred naturally over geological timescales, human activities–particularly the combustion of fossil fuels, land-use changes, and industrial emissions–have accelerated global warming at an unprecedented rate through elevated GHG concentrations (IPCC, 2023; World Energy Council, 2024). In this context, a rapid and sustained transition toward renewable energy sources and low-carbon technologies are essential to mitigate the most severe climate impacts (IEA, 2024a, IEA, 2024b).

For over a century, fossil fuels have dominated the global energy landscape, with coal, oil, and natural gas providing the majority of primary energy (Energy Institute, 2024). Among these, diesel fuel–derived from crude oil–plays a pivotal role in transportation, powering compression ignition (CI) engines used in light- and heavy-duty vehicles, maritime vessels, railway systems, and stationary industrial machinery (Energy Institute, 2024; Eurostat, 2024a; Eurostat, 2024b). As of 2023, fossil fuels still accounted for approximately 80% of global energy consumption (Energy Institute, 2024), with diesel engines responsible for about 70% of petroleum usage in Europe, equivalent to roughly 245 million tonnes of oil equivalent (Reitz et al., 2019, Eurostat, 2025).

Green diesel–also known as renewable diesel–is a mixture of diesel-compatible n-alkanes derived from fatty biomass, and it has emerged as a particularly promising substitute for fossil-derived diesel (Lucantonio et al., 2023). Unlike conventional biodiesel (fatty acid methyl esters, FAME), which must be blended with fossil diesel due to compositional differences, green diesel consists of straight-chain alkanes that are chemically indistinguishable from those in petroleum diesel (Moser, 2009; Mahdi et al., 2021). This structural compatibility allows green diesel to integrate seamlessly into existing fuel infrastructure

* Corresponding author:
Sonia Dell'Aversano
email: sonia.dellaversano@graduate.univaq.it

https://doi.org/10.31025/2611-4135/2025.19545

while potentially reducing lifecycle GHG emissions (Mahdi et al., 2021; Douvartzides et al., 2019, Mahmoudi et al., 2017).

Green diesel is produced through a catalytic deoxygenation (DO) process (Figure 1), in which triglycerides are converted into hydrocarbons via hydrogen-assisted cracking and saturation, yielding products that can be directly used in CI engines.

In the DO process, triglycerides (TGs) are catalytically converted with H_2 to produce linear n-alkanes and various byproducts (Lucantonio et al., 2023; Mahdi et al., 2021; Douvartzides et al., 2019; Di Vito Nolfi et al., 2021). The reaction pathway typically begins with the hydrogenation of TG double bonds, followed by hydrogenolysis, which cleaves ester bonds to form propane (C_3H_8) and saturated free fatty acids (FFAs, R-COOH). These FFAs are then converted into alkanes through three competing reaction mechanisms: hydrodeoxygenation (HDO), decarbonylation (DCO), and decarboxylation (DCO_2), illustrated in Equations (1–3) (Lucantonio et al., 2025; Di Vito Nolfi et al., 2021; Nugraha et al., 2024):

- HDO:
$$R{-}COOH + 3H_2 \rightarrow R{-}CH_3 + 2H_2O \quad (1)$$
- DCO:
$$R{-}COOH + H_2 \rightarrow R'{-}H + CO + H_2O \quad (2)$$
- DCO_2:
$$R{-}COOH \rightarrow R'{-}H + CO_2 \quad (3)$$

Among these, HDO is the most desirable pathway in terms of atom economy, as it retains the full carbon chain of the FFA and produces only water as a byproduct. In contrast, DCO and DCO_2 each lead to a one-carbon loss per molecule, forming carbon monoxide (CO) and carbon dioxide (CO_2), respectively (Lucantonio et al., 2025; Lin et al., 2023a; Lin et al., 2023b; Srifa et al., 2014). When long-chain fatty acids (C_{16}-C_{24}) undergo deoxygenation, the resulting n-alkanes (C_{15}-C_{18}) closely mimic fossil diesel in terms of cetane number and energy density, ensuring compatibility with conventional diesel engines. Nevertheless, side reactions such as cracking and isomerization may also occur, leading to the formation of shorter-chain or branched iso-alkanes, which can influence cold-flow behavior and combustion properties (Choudhary & Phillips, 2011; Choo et al., 2020).

The DO process typically operates at temperatures between 250-450°C and hydrogen pressures ranging from 1 to 300 bar in the presence of a solid catalyst that promotes C-O bond cleavage and hydrocarbon formation (Naqvi et al., 2023).

Both noble metals (e.g., Pd, Pt, Rh, Ru) and non-noble metals (e.g., Ni, Mo, Zn, Co) have been investigated as catalysts. Noble metals generally offer superior catalytic activity and selectivity, but their high cost limits their scalability. Consequently, industrial DO processes often favor Ni- and Mo-based catalysts, commonly supported on materials such as alumina, silica, titania, zeolites, or activated carbon (Lucantonio et al., 2023; Lucantonio et al. 2025; Upadhyay & Das, 2022; Siraj & Ceylan, 2025).

It is important to emphasize that, from a life cycle assessment (LCA) perspective (IEA, 2024c), green diesel can be considered truly sustainable only if the triglyceride feedstock, the hydrogen source and the energy needed to carry out the system are renewable. In general, green diesel qualifies as a biofuel when it is derived from biological sources–such as vegetable oils, waste cooking oils, animal fats, or algae oils–that effectively recycle atmospheric CO_2 through photosynthesis (Cherwoo & Gupta, 2023; Raman et al., 2025; Asase et al., 2024). Likewise, hydrogen sustainability is a critical factor: only electrolytic hydrogen (e-H_2), preferably generated via renewable electricity (e.g., wind or photovoltaic power), ensures a low-carbon footprint (Con-

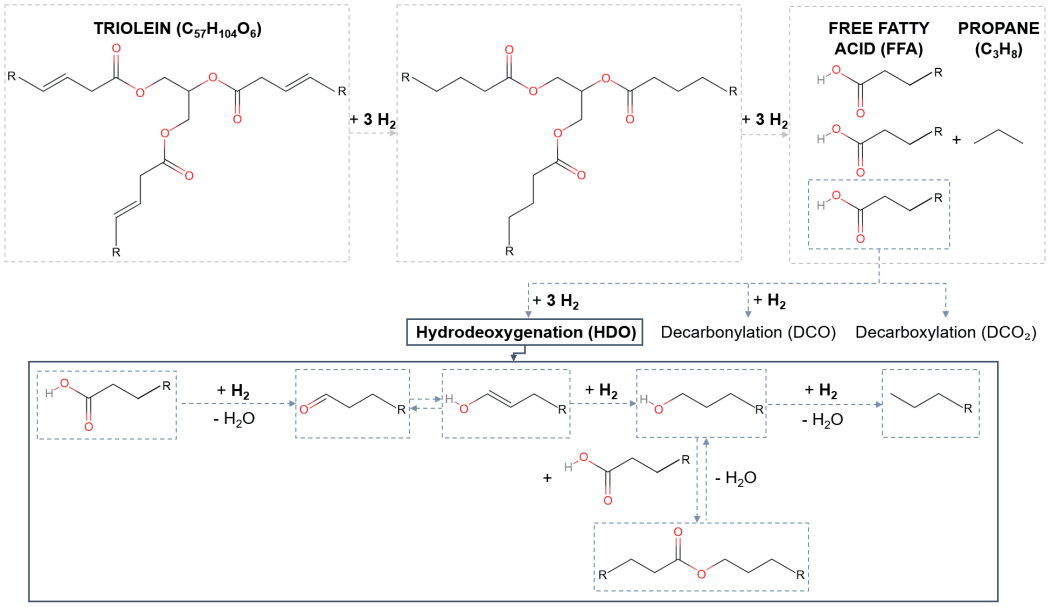

FIGURE 1: Deoxygenation process for green diesel production considering triolein as feedstock, with a focus on the hydrodeoxygenation (HDO) process.

cawe, 2024; Dell'Aversano et al., 2024; Ababneh & Hameed, 2022). Therefore, for green diesel to have a meaningful impact on GHG reduction, it must be produced as an e-biofuel–that is, a fuel made entirely from renewable feedstock and green hydrogen.

From the perspective of LCA (IEA, 2024c), in the light of the 12 principles of Green Chemistry and 12 principles of Green Engineering, the sustainability of green diesel production does not depend only on the feedstock selection; the features of the production process (DO) might be quite influential too, e.g., solvent usage.

In DO reactions, solvents not only serve as the reaction medium but also contribute to thermal stability, enhance mass transfer, and promote effective contact between reactants and catalysts. Solvent choice can markedly affect reaction kinetics, fuel quality, and process efficiency (Goh et al., 2024). Non-polar solvents like n-hexane are typically employed to reduce the viscosity of the feedstock and facilitate homogeneous mixing (Goh et al., 2024). However, the widespread use of organic solvents raises ecological and safety concerns due to their volatility, flammability, and the generation of post-reaction waste (Buldyrev et al., 2015, Kordouli et al, 2024). From a sustainability standpoint, minimizing solvent consumption per unit of fuel produced is a priority. Lower solvent usage translates to reduced operating costs, minimized emissions from solvent recovery, and less environmental risks during handling and disposal.

This study addresses the solvent-related sustainability issue by conducting a series of batch-scale DO experiments aimed at reducing the solvent-to-feedstock ratio (n-hexane:rapeseed oil mass ratio) while maintaining acceptable reaction performance. A Ni-Mo-Al catalyst synthesized through a solvent-free method was used, contributing further to the green credentials of the process. To date, most studies on green diesel synthesis have focused either on solvent-assisted deoxygenation using conventional catalysts or on novel catalyst synthesis without addressing solvent minimization (Lucantonio et al., 2023; Goh et al., 2024; Lin et al., 2023a; Nugraha et al., 2024; Mahmoudi et al., 2017). Other works have examined the influence of solvent type and quantity on the deoxygenation process (Qu et al., 2021; Maglinao et al., 2024; Zhang et al., 2024; Saleheen et al., 2019; Behtash et al., 2014). Recent advances in catalyst design for biofuel upgrading have also explored innovative preparation and activation routes, such as microwave-assisted synthesis, immobilized or supported ionic liquids, and task-specific functionalization. These strategies aim to enhance catalytic efficiency, stability, and recyclability by tailoring the microenvironment of active sites and improving mass transfer properties. A comprehensive overview of these emerging systems and their potential for biofuel upgrading is provided by recent reviews (e.g., Osman et al., 2023), which highlight their capacity to achieve high space–time yields and durable performance. However, the combined evaluation of a catalyst synthesized via a solvent-free route, together with systematically reduced solvent usage during the DO reaction, has received very limited attention. The present study specifically addresses this gap by exploring the synergy between solvent-saving approach in catalyst design and in the deoxygenation process.

A series of catalytic DO tests was performed under controlled laboratory conditions to assess the feasibility of solvent minimization without compromising product quality or deoxygenation efficiency.

2. MATERIALS AND METHODS

2.1 TG feedstock and DO catalyst

Commercial rapeseed oil was used as the triglyceride (TG) feedstock for all experiments. Its detailed composition is available in previous studies (Lucantonio et al., 2025).

The catalyst employed–referred to as Mixed Oxides by Milling (MOM)–is a powdery solid based on oxides of nickel (Ni), molybdenum (Mo), and aluminum (Al). It was synthesized through a two-step solvent-free procedure: (i) calcination of precursor salts to form individual oxides, followed by (ii) mechanical mixing of the resulting oxides via milling.

This synthesis method and MOM formulation are original and therefore currently under a patenting procedure, with related documentation reporting additional catalyst features (Di Giuliano et al., 2023; Patent No. 102023000023556).

The solvent-free synthesis was designed to achieve a nominal of equivalent NiO between 10-30 wt%, equivalent MoO_3 between 30-80 wt%, equivalent Al_2O_3 between 10-40 wt%. These results confirmed that the synthesis successfully attained the target stoichiometry. The textural properties of the material were characterized by N_2-physisorption using BET (Brunauer-Emmett-Teller) and BJH (Barret-Joiner-Halenda) analyses: the MOM catalyst exhibited a specific surface area of 35 m²/g, a pore volume of 0.06 cm³/g, and an average pore diameter of 4 nm.

Particle size distribution (PSD), determined by laser diffraction (Malvern Mastersizer 2000), showed a bimodal profile with peaks between 0.3-3 µm (maximum ≈ 0.8 µm) and 3-600 µm (maximum ≈10 µm). Cumulative PSD percentiles were: ≈0.6 µm (10^{th} percentile), ≈5.9 µm (50^{th} percentile), and ≈56.1 µm (90^{th} percentile). The Sauter mean diameter was ≈2 µm, consistent with the ball-milling process.

2.2 Experimental setup and procedure

All catalytic deoxygenation (DO) were conducted using a PARR® 4598 Mini Batch Reactor equipped with a 100 mL stainless steel vessel suitable for high-pressure operations. This setup allowed precise control of temperature, hydrogen pressure, and stirring rate–key parameters for the DO process.

Reaction conditions were selected based on methodologies reported in the literature (Lucantonio et al., 2025; Di Vito Nolfi et al., 2021) and are summarized in Table 1.

Before each run, the catalyst was pre-reduced in situ at 320°C for 4 hours under an initial hydrogen pressure of 60 bar (measured at room temperature).

DO reactions were conducted using n-hexane as the solvent, with n-hexane:oil mass ratios ($R_{S|O}$) ranging from 10:1 to 4:1. The initial oil mass (m_{oil}) varied from 2 g to 5 g,

TABLE 1: Experimental reaction conditions (RT*: Room Temperature).

Reaction parameters	Value
Temperature (T) [°C]	320
Catalyst/oil mass ratio (γ) [%]	10
Starting P(H_2) (RT*) [bar]	40
Impeller rotation [rpm]	600
Reaction time [h]	6

with the goal of increasing oil load per batch and thereby enhancing productivity.

At the end of each experiment, the catalyst was separated by filtration, and the solvent (n-hexane) was removed by rotary evaporation, leaving the final liquid product whose mass ($m_{product}$) was recorded.

The composition of the liquid product was determined via gas chromatography (GC), as described in Lucantonio et al., 2025. Peak areas ($A[\%]_p$) were quantified for the following product (p) categories:

- C_i: n-alkanes with i carbon atoms (e.g., C_{15}-C_{18})
- FAME: unconverted TG, secondarily transformed into FAME during analytical preparation
- UHC: unsaturated hydrocarbons
- BHC: branched hydrocarbons
- Others: unidentified components

2.3 DO performance metrics

To evaluate the DO process performance, the following metrics were calculated from experimentally measured quantities (Lucantonio et al., 2025; Kaewchada et al., 2021; Ruangudomsakul et al., 2021; Sonthalia & Kumar, 2019; Nugraha et al., 2024):

Product yield ($Y_{product}$, Equation 4), i.e., percentage share of the initial mass of oil (m_{oil}) that is found as a liquid product ($m_{product}$) at the end of each test:

$$Y_{product} = \frac{m_{product}}{m_{oil}} \cdot 100 \quad (4)$$

Triglyceride conversion (x, Equation 5), i.e., the percentage share of initial oil mass converted into hydrocarbons (C_i, UHC, BHC):

$$\chi = \left(1 - \frac{m_{product} \cdot \left(\frac{A[\%]_{FAME} + A[\%]_{Others}}{100}\right)}{m_{oil}}\right) \cdot 100 \quad (5)$$

Diesel-range hydrocarbon yield (Y_{diesel}, Equation 6), i.e., the percentage share of initial oil mass converted into diesel hydrocarbons C_{15}-C_{18}:

$$Y_{diesel} = \frac{m_{product}}{m_{oil}} \cdot \sum_{i=15}^{18} A[\%]_{C_i} \quad (6)$$

HDO vs. DCO_x selectivity ($S_{HDO/DCOx}$, Equation 7), i.e., the preference towards HDO or DCO_x paths (values importantly higher than 1 indicate a preference towards HDO; values lower than 1 indicate a preference towards C removing paths DCO and DCO_2):

$$S_{HDO/DCOx} = \frac{A[\%]_{C_{18}} + A[\%]_{C_{16}}}{A[\%]_{C_{17}} + A[\%]_{C_{15}}} \quad (7)$$

In addition, the mass-green-metric "Mass Productivity" defined by Roger A. Sheldon (Sheldon, R. A., 2018) was adapted to this case of study (MP, Equation 8): MP estimates the fraction of the total mass loaded in the reactor that became desired product (i.e., diesel) on the basis of:

$$MP = \frac{A[\%]_{C_{15}-C_{18}} \cdot m_{product}}{m_{oil} + m_{solvent} + m_{catalyst} + m_{H2}} \quad (8)$$

where $m_{solvent}$, $m_{catalyst}$, and m_{H2} are the initial masses of hexane, MOM, and hydrogen, respectively.

All metrics were derived from single experimental runs. Although replicated tests were not performed in the present work, the same PARR® 4598 batch reactor and GC–FID analytical setup described in Lucantonio et al. (2025) were used. In that study, three replicated experiments yielded in a standard deviation of approximately ±2 wt% (absolute) for diesel yield, corresponding to an overall reproducibility of about ±3% RSD. Considering the identical equipment and analytical procedures, this value is adopted as a representative estimate of uncertainty. The estimated uncertainty (±3% RSD) primarily reflects the combined reproducibility of the reactor system and GC-FID quantification, and therefore applies to all mass- and composition-based performance indicators ($Y_{product}$, x, and Y_{diesel}). In contrast, selectivity and peak-area percentages are expected to fall within a narrower analytical uncertainty of ≈ 1-2%.

2.4 Estimations of hydrogen availability and reactor filling

The 10:1 R_{SIO} with 2 g of oil was adopted from prior studies (Lucantonio et al., 2025) as a reference condition. Given the aim to minimize solvent usage and increase oil load, hydrogen availability was assessed as a critical process parameter.

The volume of the reactor occupied by liquids (V_L) was estimated by Equation 9 (assuming the ideal behavior of the mixing), where m_i and ρ_i denote the initial mass and density (at room temperature) of rapeseed oil and n-hexane:

$$V_L\,[l] = \left(\frac{m_{n-hexane}}{\rho_{n-hexane}} + \frac{m_{oil}}{\rho_{oil}}\right) \quad (9)$$

Hydrogen availability was then estimated using the ideal gas law and normalized against the minimum stoichiometric requirement for full deoxygenation, assuming triolein as a representative TG. Equation 10 defines the hydrogen coverage ratio (HCR):

$$HCR = \frac{P \cdot (V_{tot} - V_L)}{R \cdot T} \div (15 \cdot n_{triolein}) \quad (10)$$

where V_L is the volume of rapeseed oil and hexane, P and T are the initial loading pressure and temperature of H_2, R is the ideal gas constant, V_{tot} is the total reactor volume, and (15 x moles of triolein) is the estimated minimal H_2 demand for total DO (see figure 1). While triolein may slightly overestimate hydrogen demand due to its higher unsaturation, the HCR remains a useful indicator of system capacity.

3. RESULTS AND DISCUSSION

Table 2 presents the composition of the products obtained from the DO reactions. Table 3 summarizes the main performance metrics: product yield ($Y_{product}$), triglyceride conversion (x), diesel yield (Y_{diesel}), the HDO vs. DCO

TABLE 2: Product composition of DO tests as GC-FID peak-area percentages. Estimated analytical uncertainty ± 1-2 % based on instrument reproducibility (Lucantonio et al., 2025).

Entry	$R_{S|O}$	m_{oil}[g]	C_8-C_{14}	C_{15}-C_{18}	C_{19}-C_{30}	BHC	UHC	FAME
1	10:1	2	2.0	88.9	2.9	5.8	0.4	0.0
2	7:1	2	0.0	95.5	2.1	1.6	0.0	0.8
3	7:1	3	3.2	62.7	2.4	1.0	2.2	23.0
4	4:1	3	0.8	94.2	3.0	1.6	0.0	0.0
5	4:1	5	0.0	34.8	0.6	0.0	3.1	60.4

TABLE 3: Performance evaluation metrics of DO tests, including mass productivity (MP) as an indicator of material efficiency (g_{diesel}/g_{input}). Estimated experimental uncertainty ± 3 % RSD for mass- and composition-based quantities ($Y_{product}$, x, Y_{diesel}) based on Lucantonio et al. (2025).

Entry	$R_{S|O}$	m_{oil}[g]	$Y_{product}$[wt%]	x[wt%]	Y_{diesel}[wt%]	MP[g_{diesel}/g_{input}]
1	10:1	2	75.9	100.0	67.5	0,064
2	7:1	2	83.8	99.3	80.0	0,099
3	7:1	3	81.2	76.8	50.9	0,063
4	4:1	3	78.8	99.6	74.2	0,146
5	4:1	5	82.4	49.4	28.7	0,056

selectivity ratio ($S_{HDO/DCOx}$), and the mass productivity (MP) at varying n-hexane:oil mass ratios ($R_{S|O}$) and initial oil load.

The data reported in Tables 2 and 3 are illustrated in Figures 2 and 3. Figure 2 compares triglyceride conversion (x) and diesel yield (Y_{diesel}) for the three representative conditions: reference (10:1, 2 g), intermediate (7:1, 3 g), and constrained (4:1, 5 g). Figure 3 further separates the effects of the $R_{S|O}$ and oil loading. Figure 4 shows the variation of the hydrogen coverage ratio (HCR, 4a) and the reactor liquid volume fraction (V_L, 4b).

3.1 Effect of n-hexane:oil mass ratio and oil load

The reference test–based on Lucantonio et al. (2025) using other catalysts–consisted of a 10:1 $R_{S|O}$ and 2 g of rapeseed oil. Under these conditions, the MOM catalyst achieved excellent outcomes, with 100% triglyceride conversion and a diesel yield of 67.5 wt% (Table 3, Entry 1), and nearly 89% of the liquid product falling within the diesel-range (C_{15}-C_{18}) (Table 2, Entry 1). This served as a benchmark for comparative analysis.

From this starting point, progressively more constrained tests were designed to evaluate the impact of limited-solvent operation and increased oil load. A particularly demanding configuration–4:1 $R_{S|O}$ with 5 g of oil–resulted in significant performance losses (Figure 2): conversion dropped to 49.4% and diesel yield to 28.7 wt% (Table 3, Entry 5). Product composition confirmed incomplete reaction, with 60.4% of the product identified as FAMEs, and diesel-range hydrocarbons reduced to just 34.8% (Table 2, Entry 5). These losses can be associated with the lower HCR (≈0.8, Figure 4a) combined with reduced solvent

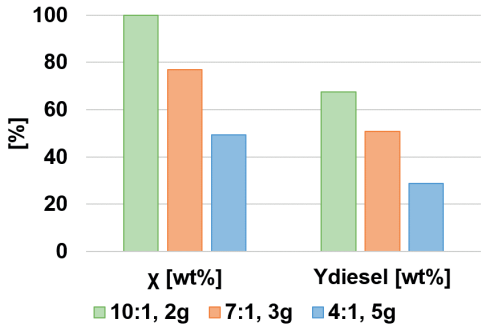

FIGURE 3: (a) Influence of n-hexane:oil mass ratio at fixed oil mass; (b) Influence of oil mass at fixed n-hexane:oil mass ratio. Estimated uncertainty ± 3 % RSD (Lucantonio et al., 2025).

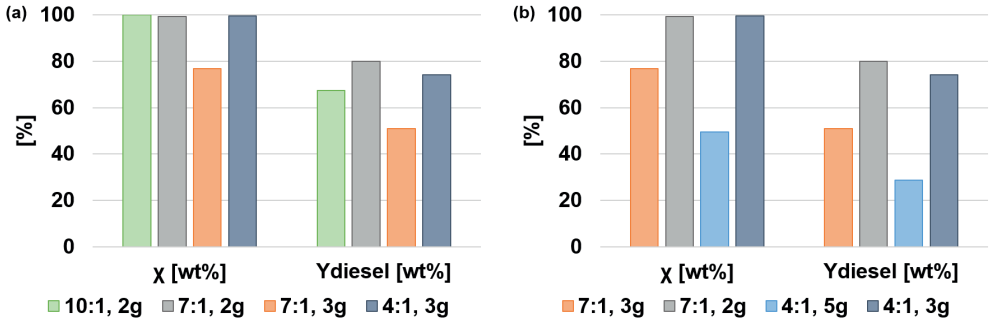

FIGURE 2: Comparison of triglyceride conversion (x) and diesel yield (Ydiesel) for the reference (10:1, 2 g), intermediate (7:1, 3 g), and constrained (4:1, 5 g) conditions. Estimated uncertainty ± 3 % RSD (Lucantonio et al., 2025).

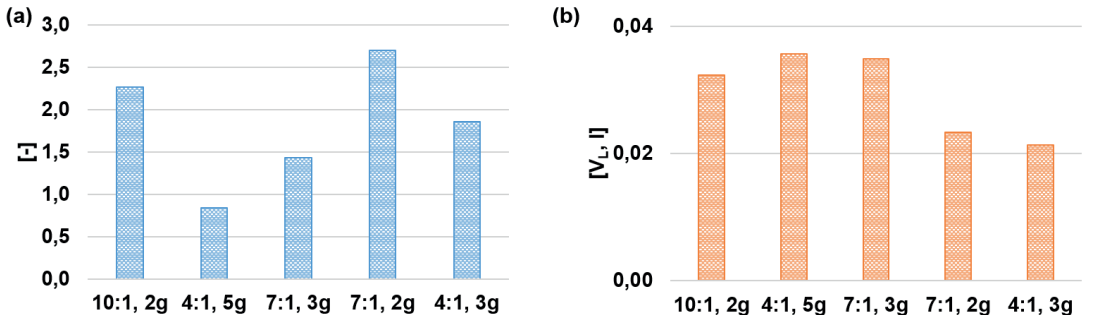

FIGURE 4: (a) estimated hydrogen coverage ratio and (b) reactor volume filled by liquids (VL) across all tested conditions.

volume. Such conditions may have limited both hydrogen availability (HCR<1) and gas-liquid mass transfer efficiency, as reported in previous studies (Maglinao et al., 2024; Žula et al., 2022; Wu et al., 2021; Saleheen et al., 2019).

To improve productivity, an intermediate test was conducted using a 7:1 $R_{S|O}$ and 3 g of oil. This configuration partially restored performance, achieving 76.8% conversion and a diesel yield of 50.9% (Table 3, Entry 3), likely due to the higher HCR (≈ 1.4, Figure 4a), which reflects greater hydrogen supply. Nevertheless, conversion and yield in this case (7:1, 3 g) did not reach the benchmark values obtained for 10:1, 2 g (Figure 2), possibly due to the lower HCR (< 1.5, Figure 4a).

Figure 3 further clarifies the separate effects of $R_{S|O}$ and oil loading. Figure 3a compares cases with equal oil loading (2 g or 3 g), while Figure 3b compares cases with equal $R_{S|O}$ (7:1 or 4:1). When the oil mass is fixed at 2 g and the $R_{S|O}$ is varied between 10:1 and 7:1, outcomes remains largely unchanged, with a slightly higher diesel yield at $R_{S|O}$ = 7:1. When the oil mass is fixed at 3 g, a noticeable improvement in both conversion and diesel yield is observed when $R_{S|O}$ decreases from 7:1 to 4:1. This can be explained by the corresponding change in HCR (Figure 4a): for 3 g of oil at $R_{S|O}$ = 7:1, the HCR is only slightly above one, indicating just sufficient hydrogen availability. However, when the solvent amount is reduced (4:1), the liquid volume (V_L) decreases (Figure 4b) and the HCR increases (to about 1.8, Figure 4a). This suggests that, within the studied range, solvent reduction can be beneficial–provided hydrogen availability remains adequate. In these experiments, an empirical threshold of HCR ≥ 1.5 (Figure 4) appears necessary to ensure satisfactory performance. Figure 3b shows that increasing the oil mass while holding a constant $R_{S|O}$ leads to a significant drop in performance. Both conversion and diesel yield decline sharply when moving from 3 g to 5 g oil at a 4:1 $R_{S|O}$, and from 2 g to 3 g at 7:1 $R_{S|O}$. These results indicate that excessive oil loading–without a corresponding increase in hydrogen–worsens DO performance. Excessive oil loading and the associated decline in conversion and yield correspond to HCR values (Figure 4a) below the empirical threshold of 1.5 identified earlier in Figure 3a. This confirms that hydrogen availability is a key factor for successful DO under the examined cases.

These observations also correlate with the differences in V_L values (Figure 4b): the two tests with the poorest performance correspond to the highest V_L values and oil loadings. Thus, while solvent reduction is feasible and even advantageous within reasonable limits, maintaining an appropriate balance between oil mass and hydrogen supply is essential to preserve reaction efficiency.

Overall, the combined comparison of Figures 2-4 suggests an interdependence between oil loading and hexane loading, both of which influence bulk hydrogen availability and hydrogen transfer through the liquid phase. Since hydrogen was preloaded in the reactor rather than continuously fed during the DO process, the actual liquid level and hydrogen partial pressure directly affect hydrogen provision to the catalyst surface. Empirically, ensuring an adequate HCR appears necessary, even though it may not be sufficient to ensure complete deoxygenation.

In summary, the 4:1 $R_{S|O}$ with 3 g of oil emerged as the compromise between process performance and solvent consumption, achieving high conversion (> 99%) and diesel yield (74.2 wt %) while substantially reducing solvent usage. This condition likely benefits from maintaining HCR well above one (empirical threshold ≈ 1.5); in constant-volume systems, this corresponds to avoiding excessive oil loading that would otherwise limit hydrogen availability.

To complement the traditional DO performance indicators, the mass productivity (MP) was calculated as in Equation 8. MP values (Table 3) varied between 0.056 and 0.146 g_{diesel}/g_{input}. Reducing the solvent-to-oil ratio from 10:1 to 7:1 (2 g oil) increased MP by over 50%, confirming that less solvent enhances atom economy. The 4:1, 3 g test exhibited the highest productivity (0.146 g_{diesel}/g_{input}), reflecting the most effective balance between solvent reduction and hydrogen supply. Conversely, further oil increase to 5 g under the same ratio led to a sharp MP decline, consistent with the drop in conversion and yield. These results emphasize that optimal productivity arises from coupling solvent reduction with sufficient hydrogen availability rather than from maximizing oil load alone.

3.2 Catalyst performance

To further evaluate the MOM catalyst's performance, product selectivity was examined for all tests made.

As shown in Figure 5a, the optimal test (4:1, 3 g) yielded over 90% diesel-range hydrocarbons (C_{15}-C_{18}), closely matching the outcome of the 7:1, 2 g experiment. In contrast, increasing the oil load to 5 g at the same $R_{S|O}$ ratio reduced this fraction to below 40%, confirming the catalyst's sensitivity to hydrogen limitation.

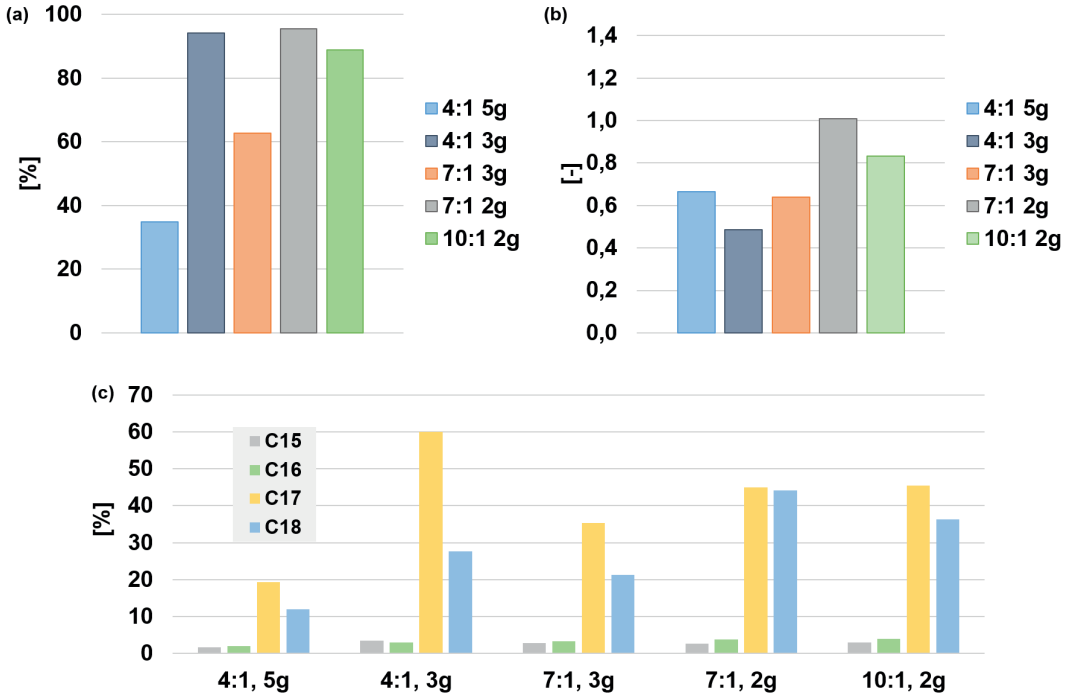

FIGURE 5: (a) A[%] of hydrocarbons in the C_{15}-C_{18} range; (b) $S_{HDO/DCOx}$ selectivity ratio; (c) detailed composition of diesel-range hydrocarbons. Analytical uncertainty within ± 1-2 % based on GC–FID reproducibility.

Selectivity data (Figure 5b) showed that the HDO/DCO_x ratio remained below 1 in all cases, indicating that decarbonylation (DCO) and decarboxylation (DCO_2) were the dominant reaction pathways. Nevertheless, higher solvent loadings and lower oil masses enhanced selectivity toward hydrodeoxygenation (HDO), suggesting a shift toward more favorable reaction routes under hydrogen-rich environments. This behavior is consistent with the stoichiometric requirements of the HDO, DCO, and DCO_x, as HDO requires a higher H_2-to-feed ratio per mole of converted fatty acid. This trend can be attributed to the combined effects of limited hydrogen solubility and restricted gas–liquid mass transfer under more constrained conditions (lower $R_{S|O}$ and higher oil loading). As the available solvent volume decreases, the effective hydrogen concentration at the catalyst surface also declines, reducing the probability of hydrogenation steps required for HDO. Consequently, the reaction preferentially follows the less hydrogen-demanding DCO/DCO_2 pathways.

Further evidence of this behavior is provided by the relative distribution of C_{17} and C_{18} hydrocarbons (Figure 5c). The formation of C_{17} species implies the loss of one carbon atom from the parent fatty chain–typical of DCO/DCO_2 routes–and their prevalence over C_{18} is a clear indicator of carbon loss. In the 4:1, 3 g case, C_{17} accounted for approximately 60% of diesel-range hydrocarbons, while C_{18} contributed only 28%, confirming dominance of decarbonation mechanisms.

Although diesel-range alkanes were the primary objective, minor amounts of light (C_8-C_{14}) and heavy (C_{19}-C_{30}) n-alkanes were also detected (Table 2). While these fractions are less valuable for direct use in CI engines, they could be further refined or valorized into other fuel streams, thereby enhancing overall process circularity and product utilization.

4. CONCLUSIONS

This work presents an experimental assessment of a more sustainable approach to green diesel production through solvent minimization during the catalytic deoxygenation of triglycerides. A novel Ni-Mo-Al catalyst, synthesized via a solvent-free procedure, was tested under varying $R_{S|O}$ ratios and oil loadings to evaluate its performance in increasingly constrained process conditions.

The results demonstrated that the reference case–$R_{S|O}$ = 10:1, 2 g of rapeseed oil–achieved complete triglyceride conversion and a diesel yield of 67.5 wt%, confirming the high activity of the MOM catalyst. As the solvent-to-oil ratio was decreased and the oil load increased, reaction outcome was significantly affected. In particular, the test conducted at a 4:1 ratio with 5 g of oil exhibited a marked decline in both conversion and diesel-range yield, along with a substantial amount of unconverted feedstock. These findings confirm the critical influence of solvent volume and process intensification on hydrogen availability and catalyst accessibility. However, an intermediate condition–4:1 $R_{S|O}$ with 3 g of oil–proved to be an effective trade-off. Here, the catalyst maintained over 99% conversion and a diesel-range hydrocarbon yield of 74.2 wt%, with more than 90% of hydrocarbons falling within the C_{15}-C_{18} range. These results demonstrate that, in a 100 mL batch reactor, solvent usage can be reduced to a 4:1 ratio while retaining acceptable yield and selectivity.

Throughout the experiments, product selectivity analysis revealed a predominance of DCO_2 and DCO pathways

over HDO, especially under hydrogen-limited environments. Nevertheless, partial HDO activity was retained, under higher solvent loadings or lower oil masses. These outcomes highlight the need for careful process balancing to ensure both fuel quality and sustainability goals.

Overall, the MOM catalyst showed strong performance and robustness under reduced solvent conditions, confirming its effectiveness for green diesel production in small-scale batch systems.

From a broader perspective, these findings represent a first step toward developing greener process designs for green diesel. Integrating solvent-free catalyst synthesis with solvent-minimized operation could ultimately reduce separation costs and enhance overall process sustainability, as gathered in evaluations in the mass-green-metric "mass productivity". Further validation under continuous-flow and pilot-scale systems will be required to translate these promising results toward industrial application.

ABBREVIATIONS

(CI) - Compression Ignition Engine
(DCO) - Decarbonylation
(DCO_2) - Decarboxylation
(DO) - Deoxygenation
(FAME) - Fatty Acid Methyl Esters
(FFA) - Free Fatty Acid
(GHG) - Greenhouse Gases
(HDO) – Hydrodeoxygenation
(LCA) – Life Cycle Assessment
(MOM) - Mixed Oxides Mill
(TGs) - Triglycerides

LIST OF SYMBOLS

($\%V_L$) - Percentage reactor filling by liquids (Equation 8)
($A[\%]_p$) - percent of area of component p in Agilent GC-FID chromatogram with p = C_i for the n-alkane with i carbon atoms; FAME for unconverted oil; UHC for unsaturated hydrocarbons; BHC for branched hydrocarbons; Others for unidentified peaks
(m_{oil}) – Initial oil mass
($m_{product}$) – Mass of recovered product
($n_{triolein}$) - Moles of triolein
(MP) – Mass productivity
(PSD) - Particle size distribution
($S_{HDO/DCOx}$) - Catalyst Selectivity (Equation 7)
(V_{tot}) - Total reactor volume
(V_L) – Reactor volume filling by liquids
(x) - Conversion of TGs (Equation 5)
(Y_{diesel}) - Diesel Yield (Equation 6)
($Y_{product}$) - Product Yield (Equation 4)

REFERENCES

Ababneh, H., & Hameed, B. H., 2022. Electrofuels as emerging new green alternative fuel: A review of recent literature. Energy Conversion and Management, 254, 115213. https://doi.org/10.1016/j.enconman.2022.115213

Asase, R. V., Okechukwu, Q. N., & Ivantsova, M. N., 2024. Biofuels: Present and future. Environment, Development and Sustainability. Advance online publication. https://doi.org/10.1007/s10668-024-04992-w

Baede, A. P. M., Ahlonsou, E., Ding, Y., & Schimel, D., 2022. The climate system: An overview. Intergovernmental Panel on Climate Change (IPCC)

Behtash, S., Lu, J., Faheem, M., & Heyden, A. (2014). Solvent effects on the hydrodeoxygenation of propanoic acid over Pd(111) model surfaces. Green Chemistry, 16, 605–616. https://doi.org/10.1039/C3GC41368C

Buldyrev, S. V., Havlin, S., & Stanley, H. E. (2015). Temporal networks: Slowing down diffusion by long lasting interactions. Proceedings of the Royal Society A: Mathematical, Physical and Engineering Sciences, 471(2184), 20150502. https://doi.org/10.1098/rspa.2015.0502

Cherwoo, L., & Gupta, I., 2023. Biofuels: An alternative to traditional fossil fuels—A comprehensive review. Sustainable Energy Technologies and Assessments, 60, 103503. https://doi.org/10.1016/j.seta.2023.103503

Choo, M. Y., Oi, L. E., Ling, T. C., Ng, E. P., Lin, Y. C., Centi, G., & Juan, J. C., 2020. Deoxygenation of triolein to green diesel in the H□-free condition: Effect of transition metal oxide supported on zeolite Y. Journal of Analytical and Applied Pyrolysis, 147, 104797. https://doi.org/10.1016/j.jaap.2020.104797

Choudhary, T. V., & Phillips, C. B., 2011. Renewable fuels via catalytic hydrodeoxygenation. Applied Catalysis A: General, 397(1-2), 1–12. https://doi.org/10.1016/j.apcata.2011.02.025

Concawe., 2024. E-Fuels: A techno-economic assessment of European domestic production and imports towards 2050 – Update (Report No. 4/24). Concawe.

Dell'Aversano S, Villante C, Gallucci K, Vanga G, Di Giuliano A., 2024 E-Fuels: A Comprehensive Review of the Most Promising Technological Alternatives towards an Energy Transition. Energies, 17(16), 3995. https://doi.org/10.3390/en17163995

Di Giuliano, A., Gallucci, K., Lucantonio, S., Rossi, L., & Di Vito Nolfi, G., 2023. Catalizzatore solido a base di ossidi di nichel, molibdeno e alluminio, per deossigenazione catalitica eterogenea di trigliceridi di origine biologica a formare idrocarburi, e suo metodo di sintesi senza solventi [Patent]. Italy. Patent Application No. 102023000023556.

Di Vito Nolfi, G., Gallucci, K., & Rossi, L., 2021. Green diesel production by catalytic hydrodeoxygenation of vegetables oils. International Journal of Environmental Research and Public Health, 18(13041). https://doi.org/10.3390/ijerph182413041

Douvartzides, S. L., Charisiou, N. D., Papageridis, K. N., & Goula, M. A., 2019. Green diesel: Biomass feedstocks, production technologies, catalytic research, fuel properties and performance in compression ignition internal combustion engines. Energies, 12(5), 809. https://doi.org/10.3390/en12050809

Energy Institute, 2024. Statistical review of world energy 2024 (73ª ed.). Energy Institute. https://www.energyinst.org/statistical-review

Eurostat, 2024a. Final energy consumption in transport - detailed statistics. European Commission. https://ec.europa.eu/eurostat/statisticsexplained/

Eurostat, 2024b. Energy statistics - an overview. European Commission. Retrieved March 9, 2025, from https://ec.europa.eu/eurostat/statistics-explained/index.php?

Eurostat, 2025. Supply, transformation and consumption of oil and petroleum products – Last update: 02/05/2025, [Online data code: nrg_bal_c]. European Commission. DOI: 10.2908/nrg_bal_c. https://ec.europa.eu/eurostat/databrowser/view/NRG_BAL_C__custom_5493868/bookmark/bar?lang=en&bookmarkId=2091c847-552d-461a-bf43-c86101de02b4

Goh, B. H. H., Chong, C. T., & Ng, J.-H., 2024. Production of Green Diesel via Solvent-aided Deoxygenation of Methyl Oleate over Bimetallic NiCo/TiO2 Catalyst. Chemical Engineering Transactions, 113, 361-366. https://doi.org/10.3303/CET24113061

International Energy Agency (IEA), 2024a. World energy outlook 2024. IEA. https://www.iea.org

International Energy Agency (IEA), 2024b. Transport sector CO□ emissions by mode in the Sustainable Development Scenario, 2000-2030. Retrieved March 9, 2025, from https://www.iea.org/data-and-statistics/charts/transport-sector-co2-emissions-by-mode-in-the-sustainable-development-scenario-2000-2030

International Energy Agency (IEA), 2024c. Towards common criteria for sustainable fuels. IEA. Retrieved from https://www.iea.org

Intergovernmental Panel on Climate Change (IPCC), 2023. Climate Change 2023: Synthesis Report. Contribution of Working Groups I, II and III to the Sixth Assessment Report of the Intergovernmental Panel on Climate Change [Core Writing Team, H. Lee, & J. Romero (Eds.)]. IPCC. https://doi.org/10.59327/IPCC/AR6-9789291691647

Kaewchada, A., Akkarawatkhoosith, N., Bunpim, D., Bangjang, T., Ngamcharussrivichai, C., & Jaree, A., 2021. Production of bio-hydrogenated diesel from palm oil using Rh/HZSM-5 in a continuous mini fixed-bed reactor. Chemical Engineering and Processing - Process Intensification, 168, 108586. https://doi.org/10.1016/j.cep.2021.108586

Kordouli, E., Lycourghiotis, S., Bourikas, K., Lycourghiotis, A., & Kordulis, C. (2024). Renewable diesel synthesis by hydro-processing in green solvents. Current Opinion in Green and Sustainable Chemistry, 48, Article 100936. https://doi.org/10.1016/j.cogsc.2024.100936

Lin, D., Mao, Z., Shang, J., Zhu, H., Liu, T., Wu, Y., Li, H. Z., Peng, C., & Feng, X., 2023a. Catalyst design strategies for deoxygenation of vegetable oils to produce second-generation biodiesel. Industrial & Engineering Chemistry Research, 62(32), 12462–12481. https://doi.org/10.1021/acs.iecr.3c01542

Lin, D., Mao, Z., Shang, J., Zhu, H., Liu, T., Wu, Y., Li, H. Z., Peng, C., & Feng, X., 2023b. Kinetic insights into deoxygenation of vegetable oils to produce second-generation biodiesel. Fuel, 333, 126416. https://doi.org/10.1016/j.fuel.2022.126416

Lucantonio S, Di Giuliano A, Rossi L, Gallucci K., 2023. Green Diesel Production via Deoxygenation Process: A Review. Energies. 16(2):844. https://doi.org/10.3390/en16020844

Lucantonio, S., Di Vito Nolfi, G., Courson, C., Gallucci, K., Di Giuliano, A., & Rossi, L., 2025. Repurposing of propane oxidative-dehydrogenation catalysts to deoxygenation of vegetable oils for green diesel production. Fuel Processing Technology, 267, 108173. https://doi.org/10.1016/j.fuproc.2024.108173

Maglinao, R. L., Taiswa, A., Davison, E. T., Andriolo, J. M., Succaw, G. L., Skinner, J. L., & Kumar, S. (2024). Role of solvent in selective hydrodeoxygenation of monomeric phenols. Biomass and Bioenergy, 189, Article 107342. https://doi.org/10.1016/j.biombioe.2024.107342

Mahdi, H. I., Bazargan, A., McKay, G., Azelee, N. I. W., & Meili, L., 2021. Catalytic deoxygenation of palm oil and its residue in green diesel production: A current technological review. Chemical Engineering Research and Design, 174, 158–187. https://doi.org/10.1016/j.cherd.2021.07.009

Mahmoudi, H., Mahmoudi, M., Doustdar, O., Jahangiri, H., Tsolakis, A., Gu, S. & LechWyszynski, M., 2017. A review of Fischer Tropsch synthesis process, mechanism, surface chemistry and catalyst formulation. Biofuels Engineering, 2(1), 11-31. https://doi.org/10.1515/bfuel-2017-0002

Moser, B. R., 2009. Biodiesel production, properties, and feedstocks. In Vitro Cellular & Developmental Biology – Plant, 45(3), 229–266. https://doi.org/10.1007/s11627-009-9204-z

Naqvi, S. R., Khoja, A. H., Ali, I., & Luque, R., 2023. Recent progress in catalytic deoxygenation of biomass pyrolysis oil using microporous zeolites for green fuels production. Fuel, 333, 126268. https://doi.org/10.1016/j.fuel.2022.126268

Nugraha, R. E., Purnomo, H., Aziz, A., Holilah, H., Bahruji, H., Asikin-Mijan, N. A., Suprapto, S., Taufiq-Yap, Y. H., Abdul Jalil, A., Hartati, H., & Prasetyoko, D., 2024. The mechanism of oleic acid deoxygenation to green diesel hydrocarbon using porous aluminosilicate catalysts. South African Journal of Chemical Engineering, 49(1), 122–135. https://doi.org/10.1016/j.sajce.2024.04.009

Osman, A.I., Elgarahy, A.M., Eltaweil, A.S., Abd El-Monaem, E.M., El-Aqapa, H.G., Park, Y., Hwang, Y., Ayati, A., Farghali, M., Ihara, I., Al-Muhtaseb, A.H., Rooney, D.W., Yap, P.-S., Sillanpää, M., 2023. Biofuel production, hydrogen production and water remediation by photocatalysis, biocatalysis and electrocatalysis. Environmental Chemistry Letters, 21, 1315–1379. https://doi.org/10.1007/s10311-023-01581-7

Qu, L., Jiang, X., Zhang, Z., Zhang, X., Song, G., Wang, H., Yuan, Y., & Chang, Y. (2021). A review of hydrodeoxygenation of bio-oil: Model compounds, catalysts, and equipment. Green Chemistry, 23, 9348–9376. https://doi.org/10.1039/D1GC03183J

Raman, R., Sreenivasan, A., Kulkarni, N. V., M, S., & Nedungadi, P., 2025. Analyzing the contributions of biofuels, biomass, and bioenergy to sustainable development goals. iScience, 28, 112157. https://doi.org/10.1016/j.isci.2025.112157

Reitz, H. R., Ogawa, H., Payri, R., Fansler, T., Kokjohn, S., Moriyoshi, Y., Agarwal, A. K., Arcoumanis, D., Assanis, D., Bae, C., Boulouchos, K., Canakci, M., Curran, S., Denbratt, I., Gavaises, M., Guenthner, M., Hasse, C., Huang, Z., Ishiyama, T., Zhao, H., 2019. IJER editorial: The future of the internal combustion engine. International Journal of Engine Research, 1–8. https://doi.org/10.1177/1468087419877990

Ruangudomsakul, M., Osakoo, N., Wittayakun, J., Keawkumay, C., Butburee, T., Youngjan, S., Faungnawakij, K., Poo-arporn, Y., Kidkhunthod, P., & Khemthong, P., 2021. Hydrodeoxygenation of palm oil to green diesel products on mixed-phase nickel phosphides. Molecular Catalysis, 523, 111422. https://doi.org/10.1016/j.mcat.2021.111422

Saleheen, M., Verma, A. M., Mamun, O., Lu, J., & Heyden, A. (2019). Investigation of solvent effects on the hydrodeoxygenation of guaiacol over Ru catalysts. Catalysis Science & Technology, 9(22), 6253–6273. https://doi.org/10.1039/C9CY01763A

Sheldon, R. A. (2018). Metrics of green chemistry and sustainability: Past, present, and future. ACS Sustainable Chemistry & Engineering, 6(1), 32–48. https://doi.org/10.1021/acssuschemeng.7b03505

Siraj, M., & Ceylan, S., 2025. Investigation of the effect of catalyst support on oleic acid catalytic deoxygenation for green diesel production. Journal of Porous Materials, 32(1), 457–469. https://doi.org/10.1007/s10934-024-01725-2

Sonthalia, A., & Kumar, N., 2019. Hydroprocessed vegetable oil as a fuel for transportation sector: A review. Journal of the Energy Institute, 92(1), 1–17. https://doi.org/10.1016/j.joei.2017.10.008

Srifa, A., Faungnawakij, K., Itthibenchapong, V., & Assabumrungrat, S., 2014. Production of bio-hydrogenated diesel by catalytic hydrotreating of palm oil over NiMoS₂/γ-Al₂O₃ catalyst. Bioresource Technology, 158, 81–90. https://doi.org/10.1016/j.biortech.2014.01.100

Upadhyay, P. R., & Das, P., 2022. Catalytic materials for green diesel production. In M. Aslam, S. S. Maktedar, & A. K. Sarma (Eds.), Green diesel: An alternative to biodiesel and petrodiesel (pp. 55–108). Springer. https://doi.org/10.1007/978-981-19-2235-0_3

World Energy Council, 2024. World energy issues monitor 2024: Redesigning energy in 5D. World Energy Council. https://www.worldenergy.org

Wu, X., Ge, Q., & Zhu, X. (2021). Vapor phase hydrodeoxygenation of phenolic compounds on group 10 metal-based catalysts: Reaction mechanism and product selectivity control. Catalysis Today, 365, 143–161. https://doi.org/10.1016/j.cattod.2020.12.033

Zhang, Z., Li, Q., Wu, X., Bourmaud, C., Vlachos, D. G., Luterbacher, J., Bodi, A., & Hemberger, P. (2024). A solution for 4-propylguaiacol hydrodeoxygenation without ring saturation. Nature Communications, 15, Article 6330. https://doi.org/10.1038/s41467-024-50724-z

Žula, M., Grilc, M., & Likozar, B. (2022). Hydrocracking, hydrogenation and hydro-deoxygenation of fatty acids, esters and glycerides: Mechanisms, kinetics and transport phenomena. Chemical Engineering Journal, 444, 136564. https://doi.org/10.1016/j.cej.2022.136564